J Therm Anal Calorim (2012) 109:1515–1523
DOI 10.1007/s10973-011-1893-y

Thermal properties of polyimide system containing silicone segments

Muhammad Bisyrul Hafi Othman · Rafiza Ramli · Zulkifli Mohamad Ariff · Hazizan Md Akil · Zulkifli Ahmad

Received: 26 May 2011 / Accepted: 26 August 2011 / Published online: 14 September 2011

Abstract The influence of the structure properties relationships of silicone incorporated polyimide (PI) on thermal stability was investigated by using single scan thermogravimetric analysis (TG) and differential scanning calorimetry (DSC) in nitrogen. Four systems have been synthesized based on monomer 4-(4-(1-(4-(4-aminophenoxy) phenyl)-1-methylethyl) phenoxy) aniline (BAPP)/ 3,3′,4,4′-Biphenyltetracarboxylic dianhydride including parent PI (S-1), PI siloxane copolymer (S-2 and S-3), and PI siloxane hybrid (S-4). The derivative thermogravimetric analysis (DTG) and DSC curves indicate a double and single stage decomposition process and glass transition temperature (T_g), respectively. While the PI, PIS, and PSH showed distinctive features towards thermal analysis, it was found that the rate of degradation ($\delta\alpha/\delta t$) was influenced by the flexibility of Si–O–Si in the backbone and in Si–O–Si itself. These results revealed that the presence of Si–O–Si in either the backbone or matrix indicates its stability with regard to high thermal service applications.

Keywords Silicone segment · Polyimide matrix · Polyimide backbone · Thermal properties · Thermal stability · Kinetic of degradation

Introduction

In the last 80 years, the synthesis of aromatic polyimides (PIs) has seen a tremendous increase within a wide range of applications, particularly in insulation materials [1, 2] and high performance polymers [3–5]. This has been due to many desirable characteristics of PI, such as excellent mechanical properties, superior chemical resistance, excellent electrical properties (low dielectric constant and high voltage breakdown), good thermal and optical properties, resistance to climate change, and its formability [6, 7]. Bruma et al. [8], and Brunchi et al. [9], reported the incorporation of flexible segmented or manipulate bulky side group into rigid PI backbone to solve the serious processing difficulties of PI; due to its extreme glass transition temperature and often, being insoluble in most organic solvents in its fully imidized form. While Cornelius et al. [10], and Wen et al. [11], reported that introducing silicone segment network into PI matrix, enhanced the excellent multifunctional properties of PI.

Chang and Wu [12] studied the degradation process of PI siloxane (PIS) copolymer in common type 3′,4,4′-benzophenone tetracarboxylic dianhydride (BTDA) with oxydianiline (ODA) using TG, and identified the structures of pyrolysis products. While Didier et al. [13], studied the thermal properties of PI Siloxane Hybrid (PSH) in a common type 4,4′-(hexafluoro-isopropylidene) diphthalic anhydride (6-FDA), 4,4′-oxydianiline (ODA-4,4′), and the 4-(allyloxy)-3-(4-aminophenoxy)phenyl amine (Al-APPA) using TG, DSC, and dynamic mechanical analysis (DMA), they also identified the structure of a sol–gel product. PI-silicone systems, which are PIS and PSH respectively, prepared through either copolymerization or via sol–gel [11, 14], require a basic understanding of structure–properties relationships (SPRs). It should be very interesting to study systematically the basics for obtaining an optimal performance PI. Furthermore, this knowledge is very useful in the investigation of estimating and distinguishing the lifetime of a PI system, either qualitatively or quantitatively. An

M. B. H. Othman · R. Ramli · Z. Mohamad Ariff · H. Md Akil · Z. Ahmad (✉)
School of Material and Mineral Resources Engineering, Engineering Campus, Universiti Sains Malaysia, Seri Ampangan, 14300 Nibong Tebal, Pulau Pinang, Malaysia
e-mail: zulkifli@eng.usm.my

additional objective of this study was to link the two methods, which were previously studied in isolation, by reviewing them together, as well as providing useful information on a wide range of related areas.

In recognizing the importance of understanding the properties of the PI, we have studied the SPRs of silicone segment incorporated PI to degradation behavior and glass transition temperature, by using single TG scan and DSC in a nitrogen atmosphere. The rate of degradation has been subsequently determined to predict the effect of silicone segment on the thermal properties of PI under two different conditions, namely; PI backbone and PI matrix. All of the PI series, derived from BAPP/BPDA monomer and siloxane segment, were incorporated into the PI backbone through copolymerization and into the PI matrix through a sol–gel process.

Experimental

Materials

Monomers used were 4-(4-(1-(4-(4-aminophenoxy) phenyl)-1-methylethyl) phenoxy) aniline (BAPP, purity > 98.0%), 3,3′,4,4′-biphenyltetracarboxylic dianhydride (BPDA, purity > 97.0%), 1,3-bis(3-aminopropyl)-1,1,3,3-tetramethyldisiloxane (DMS, purity > 95.0%), and poly (dimethylsiloxane), bis (3-aminopropyl) terminated (PDMS, purity > 95.0%) and were purchased from Sigma–Aldrich (Malaysia) Sdn Bhd. The solvents used for PI synthesis, N-methyl-2-pyrrolidinone (NMP), and tetrahydrofuran (THF), were obtained from Merck Darmstadt, Germany. The reagent used as a silica particle, tetra orthosilicate (TEOS), was also purchased from Merck Darmstadt, Germany. The chemical structures of monomers utilized, are shown in Fig. 1.

Preparation of PI films

Four series of PI were synthesized, which were S-1, S-2, S-3, and S-4 [15]. S-1 was synthesized using a conventional two-step polymerization method, while S-2 and S-3 were synthesized using a conventional three-step polymerization method. The S-4 series was prepared using a sol–gel method at ambient temperature. The final products were characterized by FT-IR to confirm the completion of the imidization process. All four series were derived from the monomers BAPP and BPDA. 10 wt% DMS and PDMS were used as a silicone segment which were then incorporated into the PI backbone. Meanwhile, 10 wt% TEOS was used as a silicone segment in the PI matrix. Mole equivalents were used for each case, while Fig. 2 summarizes the synthetic route flow to the synthesis of the four PI systems.

Characterizations and thermal analysis

The completion of imidization was amplified using a Spectrum GX Perkin Elmer Model in accordance with ASTM E 1252 [16] at a wavelength 4000–400 cm^{-1}. The PI films were purified by Soxhlet before measurements, by scanning four times. The non-isothermal thermogravimetric (TG) analysis used a Pyris 6 TGA (Perkin Elmer; Norwalk, CT, USA) in accordance with E 1131 [17] at 30 to 800 °C with a heating rate of 10 °C min^{-1} in N_2. The onset decomposition temperature (T_d), 5% mass loss temperature (T_5), 10% mass loss temperature (T_{10}), and the

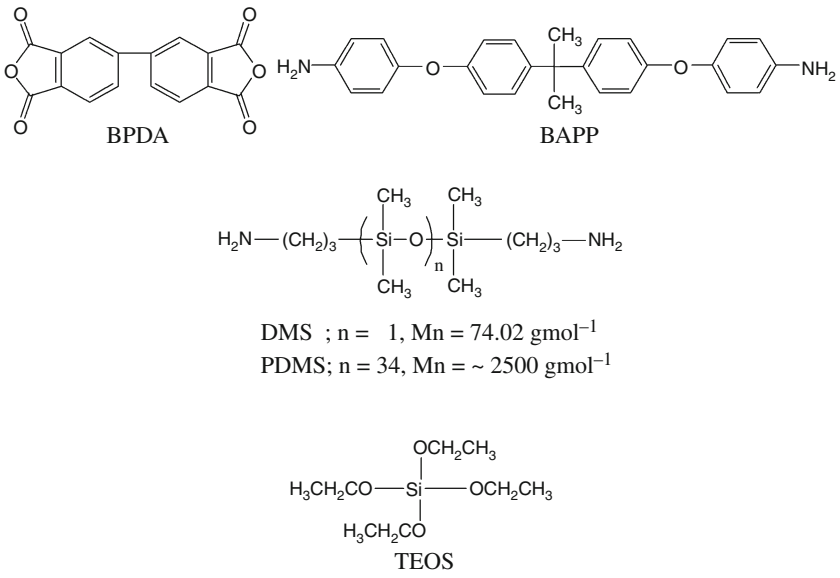

Fig. 1 The chemical structures of monomers utilized

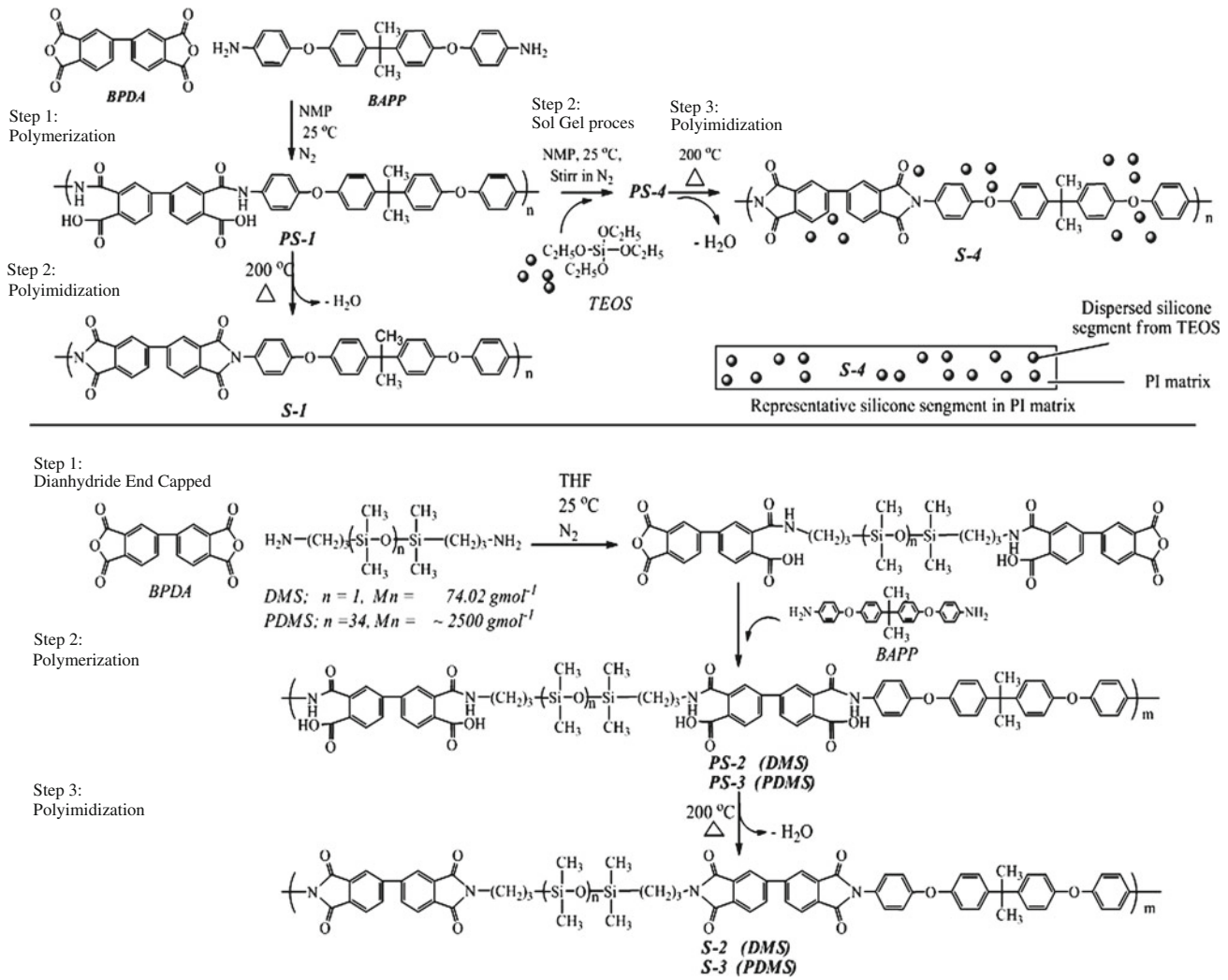

Fig. 2 The synthetic route flow to synthesis PI systems

residual mass (R_w) at 800 °C, were also determined. The non-isothermal differential scanning calorimetry (DSC) was performed using a DSC-6 analyzer (Perkin Elmer; Norwalk, CT, USA) in accordance with ASTM D3418 [18] at a heating rate of 10 °C min^{-1} in N_2, from 30 to 340 °C, to measure glass transition temperature (T_g).

Results and discussion

Characteristics of the polyimide

The preparation of the polyimide series are shown in Fig. 2. In the case of S-2 and S-3, the fixed 10 wt% of silicone segment was introduced into the PI backbone by a conventional copolymerization technique. S-2 has DMS as low molecular weight Si–O–Si segment and S-3 as high molecular weight Si–O–Si segment. Tiwari et al. [19], reported that by controlling the amount of silicone segment and the molecular mass of the silicone segment in the PI backbone, could prevent phase separation. Besides, Bushan [20] and Dieder et al. [13], reported that the incorporation of 10 wt% of silicone segment into the PI matrix via sol–gel, resulted in the phase separation between silicone segment and the PI matrix, with the silicone segment phase homogeneously dispersed throughout the PI matrix. The synthesized PI products are insoluble in conventional polar aprotic solvents, such as DMF, NMP, THF, DMAC, and DMSO, due to the rigid nature of its diimide moieties.

In our previous published study [15], the chemical structure of the synthesized PIs (S-1, S-2, S-3, and S-4) was confirmed and displayed imide characteristics, ~1720 cm^{-1} (weak, symmetric C=O imide stretch), ~1780 cm^{-1} (strong, asymmetric C=O stretch), ~1370 cm^{-1} (strong, C–N–C imide stretch), ~1100 cm^{-1}, ~740 cm^{-1} (medium, C–O–C imide ring deformation) [21–23]. While the presence of silicone segments in the PI system (S-2, S-3, and S-4) exhibited absorption at 1260 cm^{-1} ($Si\text{-}CH_3$), 1040 cm^{-1} (typical of the

stretching vibration of Si–O–Si framework from DMS and PDMS units), and 790 cm^{-1} (typical of Si–C stretching). These identical peaks are similar to those found by [8, 24, 25]. Thermal stability of PI was evaluated using TG in a nitrogen atmosphere at a heating rate of 10 °C min^{-1}, which showed major decomposition at 500 °C and determined good thermal stabilities. Meanwhile, the glass transition temperature (T_g) of PIs were determined by DSC during the second heating process from 50 to 300 °C, with a heating rate of 10 °C min^{-1} and showed exothermic peaks over 200 °C.

Thermal stability

TG analysis

TG is widely used for evaluating thermal stability and kinetic studies of polymers, due to time constraints and sample preparations. The TG and derivative thermogravimetric analysis (DTG) curves (Fig. 3) of PI series under nitrogen indicate two stages of thermal decomposition. These curves do not show mass loss below 100 °C, indicating that no water or ethanol remained in the films.

The first stage decomposition of PI series started from 300 °C and suggested, probably due to the breakdown of the flexible segments of propylidene bridge (C-$(CH_3)_2$) or siloxane (Si–O–Si), that the weakest linkages were along the polymers main chain. The second stage decomposition of PI started from 500 °C corresponding to the decomposition of the aromatic imido groups; this is typical for aromatic polyimides in general. Chen et al. [26], reported that the double-stage decomposition process of PI system, that was found in a nitrogen atmosphere, and it could be concluded that the first stage of the degradation reaction can be interpreted to the degradation of aliphatic units, and that the second stage of the degradation was mainly due to the decomposition of heterocyclic structures. Mittal and Chang et al. [27–29] reported that some of the early stages of

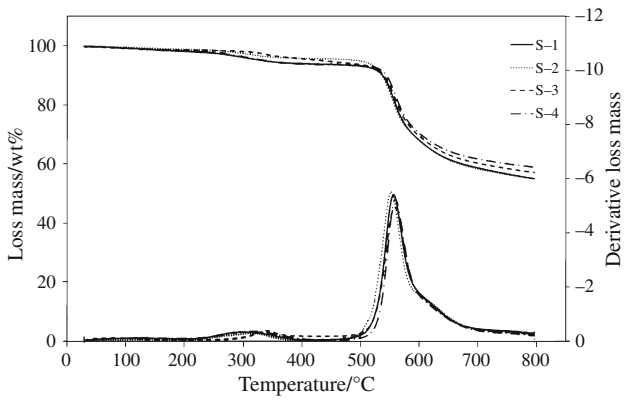

Fig. 3 TG/DTG trace for thermal decomposition of some polyimide series derived from BAPP/BPDA monomer in nitrogen atmosphere at different type silicone segment treated

double-stage decomposition could be attributed to the weak bond that may exist (–NH–, and –CONH–) between the side chain substituent and the polymer backbone. However, the resulting curve, shown in Fig. 3, indicates stable up PI series approximately 500 °C and lost approximately not less than 50% of their mass, which was illustrated in all of the synthesized PIs, had excellent stability. Chen et al. [26] and Xie et al. [30] reported that the major evolved gases during degradation are hydrocarbons, CO_2, CO, and H_2O; with hydrocarbons being evolved during the first stage of degradation (below 200 °C) as the end groups and side groups are broken from the main chain, while CO_2, CO, and H_2O are produced during the second stage of decomposition (range from 500 to 800 °C) as the main chain is broken down. However H_2O is evolved at all temperatures from around 100 °C to the very high temperature of 950 °C and this indicates that at least part of the water must be an actual product of degradation and not just adventitious moisture [30]. The polymers investigated in this study consist solely of carbon, hydrogen, nitrogen, oxygen, and silicone elements. There is more than 50% residue once the degradation is completed at 800 °C, which is mainly contributed to by un-decomposed silicon particles.

The TG characteristic decomposition temperatures of the four PI series are shown in Table 1. The onset of decomposition temperatures all followed the order S-4 > S-1 > S2, and S-3. The explanation for this is that at the onset of the decomposition temperature, the decomposition of the PI is attributed to the characteristic of the PI backbone system, where the system formed by copolymerization (S-2: BAPP-BPDA/Si–O–Si in the backbone chain) decomposes earlier than the parent PI (S-1: only BAPP-BPDA in the PI backbone). The introduction of flexible chains increases the flexibility of the polyimide backbone and thus, the loosened PI network causes chain entanglement. This will increase the chain separation and consequently facilitate the distribution of heat energy to the whole system, leading to a decrease in thermal decomposition. This may indicate that thermal decomposition starts from the flexible chains [31] and ends with the rigid chains. The introduction of flexible chains (S-3: high molecular weight Si–O–Si) enhances the flexibility of the polyimide backbone and therefore results in lower thermal decomposition. Yin et al. [31] reported that decomposition temperatures are almost independent of the length of the flexible chains and this result agrees with study reported by [32]. Meanwhile, the PI derived from the sol–gel method (S-4: Si–O-Si in the BAPP-BPDA matrix) decomposes later than the parent PI although they have a similar backbone. The increase in the thermal stability of S-4 was attributed to the high thermal stability of the silica particles (capable of holding a certain amount of heat energy) itself and the existence of a strong interaction between the silica

Table 1 Result of TG/DTG traces of some PI film in nitrogen atmosphere

Sample designation	Char residue[a]	$T_{5\%}$/°C[b]	$T_{10\%}$/°C[b]	T_{onset}/°C[c]	T_{max}/°C[d]	T_{end}/°C[e]	ΔT/°C[f]	IPDT/°C[g]
S-1	55.06	338.6	537.9	490.3	557.1	702.8	212.5	708
S-2	55.07	439.5	536.6	489.2	551.3	710.5	221.3	672
S-3	57.12	500.1	540.0	488.5	557.4	713.1	224.6	696
S-4	58.90	342.5	544.3	506.7	558.6	720.4	213.7	724

[a] wt% residue at 800 °C

[b] Temperature corresponding to percentage of mass loss

[c] Onset temperature of degradation

[d] Temperature of maximum rate of mass loss

[e] End temperature of degradation

[f] $\Delta T = T_{end} - T_{onset}$

[g] Integral procedural decomposition temperature

particles and the PI matrix. This result agrees with that reported by [33]. It can be concluded that the presence of a linkage, such as Si–O–Si in the PI backbone, contributes to the enhanced flexibility, increased molecular arrangement, and decreased thermal stabilities of the PI system [28, 34]. On the other hand, the presence of the silicone segment in the PI matrix limit the mobility of the PI chains due to the good interaction between the silicone segment and the PI chain, as well as the effects of the silica particles themselves and this further increases the thermal stability of the PI system [10].

At $T_{5\%}$ and $T_{10\%}$, the results show that the PI with silicone segment in the backbone chain had a higher thermal stability compared with the parent PI itself and that the decomposition temperature order changed, but was not apparent. Besides that, the introduction of TEOS in the PI matrix generated a Si–O–Si network which physically interacted with the PI matrix. In addition, the Si–O–Si itself, composed of high thermally conductive material [35, 36], is able to distribute heat energy to the whole structure of the PI. These contributed to the increased thermal stability of the PI systems. Unfortunately, not much study exists concerning the nature of the silicone segment in PI matrix/PI backbone, both physically and chemically. As Chen and Iroh [37] reported, there was no apparent decrease in thermal decomposition temperature of modified PI. It is generally believed that the introduction of inorganic components into organic materials can improve their thermal stability, but there might be a possible reaction between them at high temperatures, the cyclization of polyamic acid to form PI may not be complete, and this slightly (but not apparently) could change the thermal stability of the modified PI [11]. Integral procedural decomposition temperature (IPDT) was used, which sums up the shape of the TG analysis curve, and was calculated according to the method developed by Doyle [38]. The area under the TG analysis trace, from the initial temperature of 200 °C to the final temperature (T_f) of 500 °C, was determined. The ratio of this area to the total area of the rectangular plot bounded by the curve, gives A^*. The IPDT was obtained by employing the following relationship (1):

$$\text{IPDT} = A^*(T_f - T_i) + T_i \quad (1)$$

where, $T_f = 800$ °C and $T_i = 400$ °C. The IPDT values are shown in Table 1 and as expected, the IPDT was found to decrease slightly with the presence of silicone segment in the PI backbone and increase slightly with the presence of silicone segment in the PI matrix. This means that the presence of silicone segment in the PI backbone system contributed to decomposition as thermodynamic stability. Besides that, the PI, S-2, and S-3 show a large interval of decomposition temperature (ΔT). This means that the presence of silicone segment in the PI backbone system is driven to decomposition as kinetic stability.

Differential scanning calorimetry (DSC)

The glass transition temperature (T_g) of PI system, as determined from the peak of the endothermic curve in the DSC traces at second scan, were observed in the range 200–260 °C (Fig. 4). This suggests that the high T_g of PI systems are mainly attributed to the limited segment motion ability of the linking of phenyl and imide rings. It was observed that the T_g changes slightly after the introduction of silicone segment, either in the PI backbone (S-2 and S-3) or the PI matrix (S-4), in comparison to its parent PI (S-1). The DSC for all PI systems was performed in a nitrogen atmosphere at a fixed heating rate of 20 °C min^{-1}.

The DSC curve (shown in Fig. 4), of the PI series in nitrogen, showed single stages of T_g. These curves do not show an endothermic curve at 100 °C, indicating that no water remained in the films and the completion of the imidization process. The glass transition temperatures of the four PI series are shown in Table 2. These results show

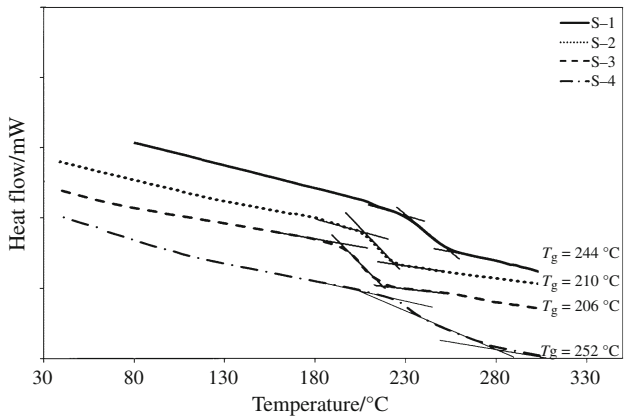

Fig. 4 DSC trace for thermal glass transition temperature T_g of some polyimide series derived from BAPP/BPDA monomer in nitrogen atmosphere at different type silicone segment treated

that the T_g of the PI series followed the order S-4 > S-1 > S2, and S-3. This can be explained by the fact that the glass transition temperatures of PI systems are particularly attributed to the characteristics of the PI in the backbone system. The system formed by copolymerization (S-2) has its transition temperature earlier than (S-1), meaning that a part of the segment in the S-2 system is capable of reacting with low heat energy to initiate a transition state. The introduction of the Si–O–Si linkage increases the flexibility of the polyimide backbone and accordingly loosens the PI network to cause chain entanglement. These enhance the separation distance between the chains and consequently raise the total free volume of the PI system. This will reduce the segmental rotational barriers and increase the segmented mobility in the PI molecules; as a result the system requires lower heat energy. This may indicate that the transition temperature originates from the flexible chains [34]. The introduction of the high molecular weight Si–O–Si (S-3) increases the flexibility of the polyimide backbone and thus enhances the respective chain separations, total free volumes, segmental motion, and molecular mobility of the system. It even gives a transition temperature that is much lower than that of S-2. Tsai [39], Whang [39], and Mayes [40] reported that the free volume is the main factor that affects the glass transition temperature.

Meanwhile, the PI derived from the sol–gel method (S-4) showed a higher transition temperature although it has a similar backbone as the parent PI. The presence of the Si–O–Si network from the sol–gel method displaces the transition temperature to higher temperatures by about ~22 °C. The increase in the transition temperature of S-4 was attributed to the high thermal stability of the silica particles (highly thermally conductive material) itself, the existence of strong interfacial interaction between the silica particles and the PI matrix and possible covalent bonding between the polyimide and TEOS. The results suggest that the mobility of the polyimide chains was restricted by the interaction of the fairly dispersed SiO_2 domains (the formation of a silica network) with the matrix polyimide. These results agree with the study reported by Zhu et al. [33] and Wang et al. [41]. Therefore, a high T_g of the polymer hybrid was observed. However, the plasticizing effect was not observed as a 10 wt% of TEOS is too much to affect it.

Apparently high ΔC_p values are shown in PI systems which contain silicone segment, whether in the backbone (copolymer S-2 and S-3) or the matrix (composite S-4), but are very characteristic of copolymer systems and composite systems. For copolymer systems, the introduction of silicone segment shows an increase in ΔC_p value. The introduction of a high molecular weight Si–O–Si (Si–O–Si length) in the PI backbone will loosen the molecular network and increase the free volume due to the chain entanglement effect. This leads to an increase in chain separation and reduces the ΔC_p value. However, this effect does not occur in the composite system. A high ΔC_p value in the composite system is attributed to the three-dimensional network of the Si–O–Si segment which is formed by silica particles. The Si–O–Si particle's high thermally conductive nature is capable of holding energy before it is distributed to the whole PI system.

Table 2 Result of DSC traces of some PI film in nitrogen atmosphere

Sample designation	T_{onset}/°C[a]	T_{mid}/°C[b]	T_{end}/°C[c]	ΔT/°C[d]	ΔC_p/J g^{-1} K^{-1}[e]
S-1	203.6	221.7	238.4	34.8	27.34×10^{-6}
S-2	191.4	207.7	224.5	33.1	42.04×10^{-6}
S-3	184.9	204.6	223.1	38.2	33.57×10^{-6}
S-4	229.6	244.1	261.9	32.3	48.12×10^{-6}

[a] Onset of transition temperature

[b] Midpoint of transition temperature

[c] End of transition temperature

[d] $\Delta T = T_{end} - T_{onset}$

[e] Delta specific heat capacity (constant pressure) at glass transition temperature

The ΔC_p value and glass transition temperature are associated by the enthalpy Eq. 2 where ΔH is an enthalpy of the PI system and ΔT is the temperature at the point of transition.

$$\Delta H = C\mathrm{p}\Delta T \tag{2}$$

Based on the DSC curve, the segmented motions of the PI molecular chains are indicated by ΔT (x-axis/°C). Increase in the flexibility of a molecule will reduce the glass transition temperature. However, at the glass transition temperature, the capability of the molecule to hold a certain amount of energy is indicated by ΔC_p (y-axis/mW). When ΔH is fixed, then ΔC_p is inversely proportional to the transition temperature for the copolymerization system.

As for S-2, S-3, and S-4, which were synthesized containing the silicone segment in the PI system, only a single T_g of significance was observed. Coleman et al. [42], reported that the miscibility component exhibited a single T_g, and therefore, the miscible T_g is the T_g between two components. Given the importance of the problem, several attempts have already been made to create a T_g equation of miscible systems. The first equation that can serve for blends as well as copolymers that are currently in use, is the Fox equation [43]; and for those for a binary system 1 + 2, we have Eq. 3.

$$\frac{1}{T_{g_p}} = \frac{x_1}{T_{g_1}} + \frac{(1 - x_1)}{T_{g_2}} \tag{3}$$

where, T_{g_p} is the pure component, and x_1 is the mass fraction of component 1. Clearly, $x_2 = 1 - x_1$. Equation 3 is symmetric with respect to the components and allows prediction from the properties of pure components only. In this way, Table 3 presents the prediction result of each PI system according to Eq. 3. The T_g obtained from Eq. 3 is almost the same as the T_g result from the DSC traces in a nitrogen atmosphere. This reinforces the assumption that the synthesized PI is a miscible system at room temperature and indicates that the PI linkage of BAPP–BPDA and silicone segment, are chemically compatible in the PI system.

The presence of a flexible Si–O–Si linkage in the PI backbone internally contributes to the flexibility of the chain molecule and creates more available free volume for molecular relaxation to lower the T_g in the x_1 system. As x_2 acts as a plasticizer, it also contributes towards lowering the T_g in the PI systems. The single T_g values obtained from the miscible "x_1 and x_2" systems suggest that a 0.1 mol fraction of silicone segment used will attribute to a chemically compatible system. However, the reduction of T_g revealed that the presence "silicone segment in the PI backbone" material is less rigid compared with the pure PI, and the "silicone segment in the PI matrix" material. The glass transition for S-3 is both lower and broader than that of S-2. This is mostly due to the presence of a longer polysiloxane segment in S-3, which rendered its higher chain flexibility. The T_g of the polysiloxane segment, which would otherwise have been detected in the DSC scan in the sub-ambient region, was not observed. This could be due to the micro-phase separation morphology, whose scale of thermal transition was too small to detect. Another plausible reason would be that the siloxane unit was tightly confined between the rigid PI chains, which limited any segmental movement to the former. As expected, no melting transition was observed for all samples within this range of temperatures.

Kinetic evaluation

Kinetic TG analysis

Generally, for the kinetics of polymer degradation, it is assumed that the rates of conversion are proportional to the concentration of the reacted material [44] and can be expressed by the basic rate Eq. 4.

Table 3 Result of some glass transition temperature of silicone segment utilized and method approached

Sample designation	Silicone segment[a]	T_{g_1}/C[b]	T_{g_2}/°C[c]	X_{2s}^{d}	Approach[e]	T_{g_1}/°C[f]
S-1	–	221.7	–	–	Control	221.7
S-2	DMS	221.7	−108.5	0.1	Copolymerization	207.7
S-3	PDMS	221.7	−121.3	0.1	Copolymerization	204.6
S-4	TEOS	221.7	164.4	0.1	Sol–gel	244.1

[a] Silicone segment which introduce into PI system

[b] Glass transition temperature of BAPP/BPDA system

[c] Glass transition temperature of silicone segment oligomer

[d] mol fraction of silicone segment component

[e] Method used

[f] Glass transition temperature from DSC trace

$$\frac{d\alpha}{dt} = k(T)f(\alpha) \quad (4)$$

where, $d\alpha/dt$ is the conversion rate, k is rate constant, and $f(\alpha)$ is a function of conversion. For TG analysis, the conversion rate of a reaction is defined as the ratio of actual mass loss to the total mass loss corresponding to the degradation process; shown by Eq. 5.

$$\alpha = \frac{M_o - M_t}{M_o - M_f} \quad (5)$$

where, M_o, M_t,, and M_f, are the initial mass of the sample, the mass of the sample at time, and the final mass of the completely decomposed sample, respectively. The conversion rate, $d\alpha/dt$, is obtained from the plot of conversion (α) against time (t), which is $d\alpha/dt$, and is the slope of the curve for each conversion (Fig. 5).

The entire sample of the PI system showed the maximum rate of decomposition around 0.4 conversions, meaning that less than 50% of the material was decomposed. It suggests that the synthesized PI is good in terms of thermal stability due to the stability of the imide linkages ability to withstand temperature [45]. At the optimum conversion region (0.3–0.5), both S-1 and S-4 showed the maximum $\delta\alpha/\delta t$ at the same α region; as well as both S-2 and S-3. This suggests that the conversion of degradation is driven by the relationship of the PI backbone structure. However, for each α, each system does not retain the $\delta\alpha/\delta t$ curve due to the micro-decomposition PI segment. More than four divisions of the α region have been identified as affecting the $\delta\alpha/\delta t$ of PI degradation. Each of the $\delta\alpha/\delta t$ PI systems is ruled by the silicon segment and is very difficult to interpret, and thus require further in-depth research. However, it can be concluded that the PI ruled by silicone segment is closely related to the solid state of the PI system, flexibility of the structure, morphology, and the presence of silicon itself. As shown in Fig. 5, at an optimum α, the $\delta\alpha/\delta t$ follows the order S-4 > S-1 and S2 > S-3. These regions, distinguishable by the $\delta\alpha/\delta t$, were attributed to the characteristics of the backbone. At the end of α, the $\delta\alpha/\delta t$ is driven by the silicone itself.

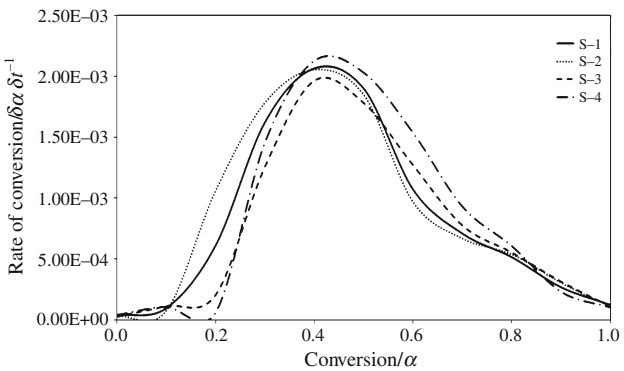

Fig. 5 The graph between conversion rate ($d\alpha/dt$) versus conversion (α) for all PI systems in nitrogen atmosphere

Conclusions

We have successfully synthesized four PI systems based on monomers 4-(4-(1-(4-(4-aminophenoxy) phenyl)-1-methylethyl) phenoxy) aniline (BAPP)/3, 3′, 4, 4′-Biphenyltetracarboxylic dianhydride (BPDA), by introducing silicone segment into two different conditions, i.e., the PI backbone and the PI matrix. The influence of the structure property relationships of silicone incorporated PI towards thermal stability, were investigated using a single scan TG and DSC, in a nitrogen atmosphere. The DTG and DSC curves indicated both a double and single stage decomposition process and glass transition temperature (T_g), respectively. The results reveal that the kinetic of degradation was influenced by the characteristics of the PI backbone system, and by the presence of silicone itself. However, it is very difficult to interpret each conversion step. It was found that the rate of degradation ($\delta\alpha/\delta t$) was influenced by the flexibility of Si–O–Si in the backbone, and Si–O–Si itself. These results revealed its stability towards high thermal service applications.

Acknowledgements The authors wish to acknowledge the USM for sponsoring this project under USM-FRGS-814069, USM-RU-PGRS 8032006, and School of Material and Mineral Source Engineering, Engineering Campus USM for technical support.

References

1. Othman M, Ahmad Z, Akil H, editors. Fabrication of nanoporous polyimide of low dielectric constant. In: Electronic manufacturing technology symposium (IEMT), 2008 33rd IEEE/CPMT international 2010; Penang IEEE.
2. Li Y, Obando N, Tschen F, Morgan R. Thermal analysis of phenylethynyl end-capped fluorinated imide oligomer afr-pepa-4. J Therm Anal Calorim. 2006;85(1):125–9.
3. Hergenrother P. The use, design, synthesis, and properties of high performance/high temperature polymers: an overview. High Perform Polym. 2003;15(1):3.
4. Torrecillas R, Baudry A, Dufay J, Mortaigne B. Thermal degradation of high performance polymers—influence of structure on polyimide thermostability. Polym Degrad Stab. 1996;54(2–3):267–74.
5. Vijayakumar CT, Surender R, Rajakumar K, Alam S. Synthesis and thermal studies of bisphenol-A based bismaleimide. J Therm Anal Calorim. 2011;103(2):693–9.
6. Ghosh A, Banerjee S. Thermal, mechanical, and dielectric properties of novel fluorinated copoly (imide siloxane)s. J Appl Polym Sci. 2008;109(4):2329–40.
7. Padmanabha Raju M, Alam S. Synthesis and thermal behaviour of silicon containing poly (ester imide)s. J Therm Anal Calorim. 2008;91(2):401–4.

8. Brum M, Sava I, Damaceanu DM, Belomoina NM, Robinson J. New polyimides containing siloxane groups in the main chain. Revue Roumaine de Chimie. 2008;53(9):803–11.
9. Brunchi C, Filimon A, Cazacu M, Ioan S. Properties of some poly (siloxane) s for optical applications. High Perform Polym. 2009; 21(1):31.
10. Cornelius C, Marand E. Hybrid inorganic-organic materials based on a 6FDA-6FpDA-DABA polyimide and silica: physical characterization studies. Polymer. 2002;43(8):2385–400.
11. Wen J, Wilkes GL. Organic/inorganic hybrid network materials by the sol–gel approach. Chem Mater. 1996;8(8):1667–81.
12. Chang T, Wu K. Characterization and degradation of some silicon-containing polyimides. Polym Degrad Stab. 1998;60(1):161–8.
13. Didier B, Mercier R, Alberola N, Bas C. Preparation of polyimide/silica hybrid material by sol–gel process under basic catalysis: comparison with acid conditions. J Polym Sci B Polym Phys. 2008;46(18):1891–902.
14. Gomes S, Margaça FMA, Ferreira L, Miranda Salvado I, Falcao A. Thermal analysis of hybrid materials prepared by-irradiation. J Therm Anal Calorim. 2009;95(1):99–103.
15. Othman MBH, Ramli MR, Tyng LY, Ahmad Z, Akil HM. Dielectric constant and refractive index of poly (siloxane-imide) block copolymer. Mater Des. 2011;32(6):3173–82.
16. Anual book of ASTM standards. Standard practice for general techniques for obtaining infrared spectra for qualitative analysis. 2007;03.06:13.
17. Anual book of ASTM standards. Standard test method for compositional analysis by thermogravimetry. 2008;14.02:5.
18. Anual book of ASTM standards. Standard test method for transition temperatures and enthalpies of fusion and crystallization of polymers by differential scanning calorimetry. 2008;08.02:7.
19. Tiwari A, Sugamoto R, Hihara L. Analysis of molecular morphology and permeation behavior of polyimide-siloxane molecular composites for their possible coatings application. Prog Org Coat. 2006;57(3):259–72.
20. Bhushan B. Springer handbook of nanotechnology, vol. 1. New York: Springer-Verlag; 2004.
21. Meng X, Huang Y, Yu H, Lv Z. Thermal degradation kinetics of polyimide containing 2,6-benzobisoxazole units. Polym Degrad Stab. 2007;92(6):962–7.
22. Hsiao S, Chen Y. Structure-property study of polyimides derived from PMDA and BPDA dianhydrides with structurally different diamines. Eur Polym J. 2002;38(4):815–28.
23. Sroog C. Polyimides. J Polym Sci Macromol Rev. 1976;11(1): 161–208.
24. Park H, Kim J, Nam S, Lee Y. Imide-siloxane block copolymer/silica hybrid membranes: preparation, characterization and gas separation properties. J Membr Sci. 2003;220(1–2):59–73.
25. Andre S, Guida Pietrasanta F, Rousseau A, Boutevin B. Novel synthesis of polyimide–polyhybridsiloxane block copolymers via polyhydrosilylation: Characterization and physical properties. J Polym Sci A Polym Chem. 2001;39(14):2414–25.
26. Chen C, Huang X, Qin W. Preparation, characterization and thermal decomposition of polyimides with main chain containing cycloaliphatic units. J Macromol Sci B. 2008;47(1):109–16.
27. Mittal K. Polyimides and other high temperature polymers: synthesis, characterization and applications. New Delhi: VSP; 2003.
28. Mittal K. Polyimides and other high temperature polymers: synthesis, characterization, and applications. Leiden: Brill Academic Pub; 2009.
29. Wang Y, Xu S, Chen T, Guo H, Liu Q, Ye B, et al. Synthesis and preliminary photovoltaic behavior study of a soluble polyimide containing ruthenium complexes. Polym Chem. 2010;1(7):1048–55.
30. Xie W, Pan WP. Thermal characterization of materials using evolved gas analysis. J Therm Anal Calorim. 2001;65(3):669–85.
31. Yin J, Ye Y-f, Wang Z-g. Study on preparation and properties of polyimides containing long flexible chains in the backbone. Eur Polym J. 1998;34(12):1839–43.
32. Marek M Jr, Labský J, Schneider B, Štokr J, Bednář B, Králíček J. Preparation and properties of polypyromellitimides prepared from 1,n-bis(4-aminophenoxy)alkanes. Eur Polym J. 1991;27(6): 487–91.
33. Zhu ZK, Yang Y, Yin J, Qi ZN. Preparation and properties of organosoluble polyimide/silica hybrid materials by sol–gel process. J Appl Polym Sci. 1999;73(14):2977–84.
34. Bacosca I, Hamciuc E, Bruma M, Ronova I, Nikitin L, editors. In: Study of polyimides containing flexible groups-IEEE; 2009.
35. Zaharescu M, Jitianu A, Braileanu A, Madarász J, Pokol G. Ageing effect on the SiO_2-based inorganic-organic hybrid materials. J Therm Anal Calorim. 2001;64(2):689–96.
36. Zaharescu M, Jitianu A, Brăileanu A, Madarász J, Novák C, Pokol G. Composition and thermal stability of SiO_2-based hybrid materials TEOS-MTEOS system. J Therm Anal Calorim. 2003; 71(2):421–8.
37. Chen Y, Iroh JO. Synthesis and characterization of polyimide/silica hybrid composites. Chem Mater. 1999;11(5):1218–22.
38. Doyle CD. Estimating thermal stability of experimental polymers by empirical thermogravimetric analysis. Anal Chem. 1961;33(1): 77–9.
39. Tsai M, Whang W. Low dielectric polyimide/poly (silsesquioxane)-like nanocomposite material. Polymer. 2001;42(9):4197–207.
40. Mayes A. Glass transition of amorphous polymer surfaces. Macromolecules. 1994;27(11):3114–5.
41. Wang L, Tian Y, Ding H, Li J. Microstructure and properties of organosoluble polyimide/silica hybrid films. Eur Polym J. 2006; 42(11):2921–30.
42. Coleman M, Kohn R, Koros W. Gas-separation applications of miscible blends of isomeric polyimides. J Appl Polym Sci. 1993; 50(6):1059–64.
43. Fox T. Influence of diluent and of copolymer composition on the glass temperature of a polymer system. Bull Am Phys Soc. 1956;1(123):22060–6218.
44. Tiptipakorn S, Damrongsakkul S, Ando S, Hemvichian K, Rimdusit S. Thermal degradation behaviors of polybenzoxazine and silicon-containing polyimide blends. Polym Degrad Stab. 2007; 92(7):1265–78.
45. Keller T. Imide-containing phthalonitrile resin. Polymer. 1993; 34(5):952–5.